

**To cite this article:** ZHANG Q W, YU X, YANG L H. Multi-line spectrum feedback control algorithm for active vibration isolation [J/OL]. Chinese Journal of Ship Research, 2021, 16(6). <http://www.ship-research.com/EN/Y2021/V16/I6/132>.

**DOI:** 10.19693/j.issn.1673-3185.02107

# Multi-line spectrum feedback control algorithm for active vibration isolation



ZHANG Qingwei<sup>1</sup>, YU Xiang<sup>\*2</sup>, YANG Lihua<sup>3,4</sup>

<sup>1</sup> College of Power Engineering, Naval University of Engineering, Wuhan 430033, China

<sup>2</sup> College of Naval Architecture and Ocean Engineering, Naval University of Engineering, Wuhan 430033, China

<sup>3</sup> Power Control Department, Naval Submarine Academy, Qingdao 266199, China

<sup>4</sup> Key Laboratory of Noise and Vibration Research, Institute of Acoustics, Chinese Academy of Sciences, Beijing 100190, China

**Abstract:** [Objectives] Considering the poor control effect of the traditional adaptive filtering algorithm for multi-frequency excitation in vibration control and the engineering problems that difficult sensor installation and channel coupling cause reference signal mismatch, this paper proposes a multi-line spectrum feedback control algorithm. [Methods] First, the error signal passes through the cascaded adaptive notch filters, and the notch filter parameters are updated according to the adaptive algorithm to estimate multiple signal frequencies. Next, each reference signal is synthesized, phase compensation is performed, and another reference signal is obtained through the Hilbert transform. Finally, the signals enter parallel controllers to complete the amplitude update and thereby achieve vibration control. [Results] Through simulation and experimental verification, the results show that the proposed algorithm can accurately estimate frequency information, synthesize reliable reference signals, and achieve 20 – 40 dB energy attenuation for 30, 37, 60, 110 Hz line spectra. [Conclusions] This algorithm provides a better solution to the problems of reference signal mismatch and multi-line spectrum vibration in vibration control and effectively reduces and suppresses low-frequency vibration energy transmission.

**Key words:** multi-frequency excitation; reference signal mismatch; active vibration isolation; vibration control; adaptive notch filter; frequency estimation; Hilbert transform

**CLC number:** U661.44; TB535.1

## 0 Introduction

The vibration generated by the operation of a ship's mechanical equipment forms complex low-frequency line spectrum noises in seawater [1], and this type of noise is the major target feature for anti-submarine equipment to detect. Active vibration isolation is able to effectively suppress low-frequency vibration, and many relevant studies have been carried out at home and abroad [2-4].

In the algorithm field, the conventional filter-X least mean square (FXLMS) algorithm has been ex-

tensively used [5] because of its simple structure and easy implementation. However, it is difficult for this algorithm to achieve effective control in the case of complex multi-line spectrum excitation. For this reason, Zhao et al. [6] proposed a frequency-selective active control algorithm that achieved the control of multiple line spectra by constructing a two-level orthogonal filter structure. Li et al. [7] put forward a multi-channel narrow-band Fx-Newton control algorithm that used a band-pass filter to extract multiple line spectra for separated control. Gao et al. [8] presented a variable-step adaptive wavelet

**Received:** 2020 – 09 – 08

**Accepted:** 2020 – 10 – 18

**Supported by:** National Natural Science Foundation of China (51679245, 51909267); Shandong Provincial Natural Science Foundation (ZR2019QEE031)

**Authors:** ZHANG Qingwei, male, born in 1994, master degree candidate. Research interest: active vibration control.

E-mail: 2923172134@qq.com

YU Xiang, male, born in 1978, Ph.D., associate professor. Research interest: noise and vibration control.

E-mail: yuxiang898@sina.com

**\*Corresponding author:** YU Xiang

packet algorithm, which decomposed the collected signal into different frequency bands to achieve multi-frequency signal control. However, the aforementioned algorithms all rely on reference signals with precise frequencies. Engineering problems such as difficult sensor installation and channel coupling make it difficult to collect reference signals or produce errors in such signals, i.e., reference signal mismatch, thereby influencing the control effect. In response, Zhang et al. [9] proposed a scheme for obtaining signal frequency by measuring the signal autocorrelation sequence. Zhai et al. [10] suggested the use of the fast Fourier transform (FFT) method for signal spectrum estimation. Nevertheless, these algorithms all face the problem of large estimation errors, making it difficult to synthesize reference signals with a high signal-to-noise ratio (SNR). Studies show that frequency estimation methods based on adaptive notch filters can be employed for accurate line spectrum control and that their band-notched characteristics are suitable for this application [11-13].

In light of the above studies, this paper proposes a multi-line spectrum feedback control algorithm based on adaptive notch filters. Specifically, the error signal passes through cascaded adaptive notch filters, and the notch filter parameters are updated according to the adaptive algorithm to estimate multiple signal frequencies. Phase compensation is per-

formed, and each reference signal is synthesized. Then, the Hilbert transform is applied to the signal to obtain another reference signal. Finally, the signals enter the parallel controllers for amplitude update and the suppression of multi-line spectrum vibration, thereby solving the problem of reference signal mismatch.

## 1 Multi-line spectrum feedback control algorithm

### 1.1 Principle of notch filter

A notch filter is a special band-stop filter that can be used to strip specific frequency components, and it exhibits a minor impact on other frequency components. Fig. 1(a) shows its amplitude-frequency characteristics. The structure of a notch filter can usually be expressed by a second-order infinite impulse response (IIR) filter with a transfer function of

$$H(z) = \frac{1 + a \cdot z^{-1} + z^{-2}}{1 + r \cdot a \cdot z^{-1} + r^2 \cdot z^{-2}} \quad (1)$$

where  $a$  is a parameter related to the normalized notch frequency;  $r$  is a constant smaller than but close to 1 that affects the 3 dB notch bandwidth. In particular, a larger  $r$  results in a narrower notch opening, i.e., a smaller 3 dB bandwidth and a better effect. The variation of notch amplitude (the amplification factor of the notch filter) with  $r$  is shown in Fig. 1(b).

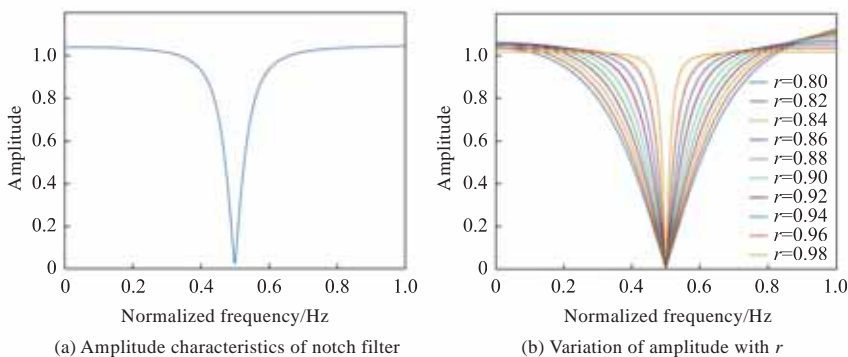


Fig. 1 Structure of IIR notch filter

Two basic conditions need to be satisfied to achieve notch: The zeros of the transfer function have to be on the unit circle so that the trap depth at the notch frequency is infinite; the poles of the function should match the zeros in the way that other frequency components are not affected. The zero-pole distribution is shown in Fig. 1(c), and the relationship between a pole-zero pair  $p_i$  and  $z_i$  is

$$p_i = r \cdot z_i \quad (2)$$

It is assumed that there is a pair of conjugate zeros  $z_{1,2} = e^{\pm j\omega_0}$  at the angles of  $\pm\omega_0$  traveled per unit time on the  $z$ -plane. According to Eq. (2),  $p_{1,2} = r \cdot e^{\pm j\omega_0}$  can be obtained, and its transfer function can be expressed as

$$H(z) = \frac{(z - e^{j\omega_0}) \cdot (z - e^{-j\omega_0})}{(z - r \cdot e^{j\omega_0}) \cdot (z - r \cdot e^{-j\omega_0})} = \frac{1 - (2 \cdot \cos \omega_0 \cdot z^{-1}) + z^{-2}}{1 - (2 \cdot r \cdot \cos \omega_0 \cdot z^{-1}) + r^2 \cdot z^{-2}} \quad (3)$$

Matching the coefficients of Eq. (1) and Eq. (3)

leads to

$$a = -2 \cos \omega_0 \quad (4)$$

## 1.2 Frequency estimation

According to the relationship between the relevant parameter  $a$  of the transfer function of the notch filter and the angular frequency  $\omega_0$  in Eq. (4), a specific frequency can be identified and extracted by setting  $a$ . For no influence of the upper-level notch filter's estimation error on lower-level frequency estimation, the error  $\varepsilon_i(n)$  of the notch filter at each level is employed to regulate the parameter  $a_i(n)$  ( $n$  is the number of iterations) of its transfer function to ensure an accurate estimation of the excitation frequency. The structure of the  $N$ -level cascaded adaptive notch filters is shown in Fig. 2, in which  $k$  is the  $k$ -th notch filter and  $v_k(n)$  is the input signal for the notch filter of each level.

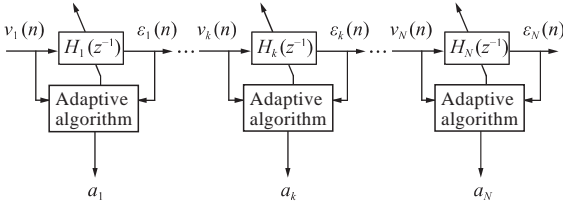


Fig. 2 Structure of  $N$ -level cascaded adaptive notch filters

According to the adaptive algorithms, the iterative formula can be written as follows.

$$a_i(n+1) = a_i(n) - \mu_i \nabla_i(n) \quad (5)$$

where  $\mu_i$  is the iteration step size;  $\nabla_i(n)$  is the gradient operator for the mean square error expressed as

$$\nabla_i(n) = \frac{\partial [\varepsilon_i^2(n)]}{\partial a_i} = 2\varepsilon_i(n) \frac{\partial \varepsilon_i(n)}{\partial a_i} \quad (6)$$

According to the input-output relationship in Eq. (1), the following equation can be obtained:

$$\varepsilon_i(n) = \frac{1+a_i(n)z^{-1}+z^{-2}}{1+ra_i(n)z^{-1}+r^2z^{-2}} \cdot v_i(n) \quad (7)$$

Expanding Eq. (7) leads to

$$\begin{aligned} \varepsilon_i(n) + ra_i(n)\varepsilon_i(n-1) + r^2\varepsilon_i(n-2) = \\ v_i(n) + a_i(n)v_i(n-1) + v_i(n-2) \end{aligned} \quad (8)$$

The partial derivative of Eq. (8) with respect to  $a_i(n)$  is solved to obtain the following equation:

$$\begin{aligned} \frac{\partial \varepsilon_i(n)}{\partial a_i} + ra_i(n) \frac{\partial \varepsilon_i(n-1)}{\partial a_i} + r\varepsilon_i(n-1) + \\ r^2 \frac{\partial \varepsilon_i(n-2)}{\partial a_i} = v_i(n-1) \end{aligned} \quad (9)$$

The formulae for line spectrum frequency (LSF) estimation can be obtained by combining Eq. (5) through Eq. (9)

$$a_i(n+1) = a_i(n) - \mu_i v_i(n-1) \tilde{\varepsilon}(n) \quad (10)$$

$$\tilde{\varepsilon}(n) \approx \frac{1}{1+ra_i(n)+r^2} \left( 1 - \frac{\varepsilon_i(n-1)}{v_i(n-1)} \right) \quad (11)$$

## 1.3 Narrow-band line spectrum control algorithm

Hard reference signal collection and large SNR are adverse to the employment of the feedback algorithm or effective vibration control. The response of a linear time-invariant (LTI) system (the primary channel  $P(z)$  is an LTI system) is characterized by frequency retention when an excitation signal passes through it. Therefore, adaptive control can be achieved by extracting frequency information from error signals on the basis of a feedback control structure.

The proposed algorithm is shown in Fig. 3. This algorithm means to pass the error signal through cascaded adaptive filters and output  $a_i(n)$ , which then enters the signal synthesizer. In this algorithm, phase is also crucial to the implementation of vibration control. In the case of an error with respect to the phase of the reference signal, the control effect of the algorithm is poor or even invalid, and phase compensation should thus be applied to the synthesized signal. The reference signal  $x_{i1}(n)$  is adjusted by the second-order autoregressive model<sup>[14]</sup>, i. e., Eq. (12) is employed to estimate the phase of an unknown reference signal.

$$x_{i1}(n) = a_i(n)x_{i1}(n-1) - x_{i1}(n-2) \quad (12)$$

Meanwhile, the Hilbert transform is applied to the reference signal  $x_{i1}(n)$  to obtain another reference signal  $x_{i2}(n)$

$$x_{i2}(n) = H[x_{i1}(n)] = \int_{-\infty}^{+\infty} \frac{x_{i1}(\tau)}{\pi(n-\tau)} d\tau \quad (13)$$

where Hilbert transform  $H[x_{i1}(n)]$ , an LTI system with an impulse response of  $h(t)=1/\pi t$ , is an all-pass filter that achieves a  $90^\circ$  phase shift and is suitable for narrow-band signals;  $\tau$  is the integral variable.

The two synthesized reference signals enter the control filter respectively for amplitude update, and the output signal is expressed as

$$y_i(n) = w_{i1}(n)x_{i1}(n) + w_{i2}(n)x_{i2}(n) \quad (14)$$

where  $w_{i1}(n)$  is the weight coefficient vector of the  $i$ -th controller.

The total output of each control unit is

$$y(n) = \sum_{i=1}^N [w_{i1}(n)x_{i1}(n) + w_{i2}(n)x_{i2}(n)] \quad (15)$$

The residual signal  $e(n)$  is

$$e(n) = d(n) - \sum_{j=0}^{M-1} s_j \cdot y(n-j) \quad (16)$$

where  $d(n)$  is the desired signal;  $s_j$  stands for the  $M$ -order coefficient of the real secondary channel.

In practice, the transfer characteristics of the sec-

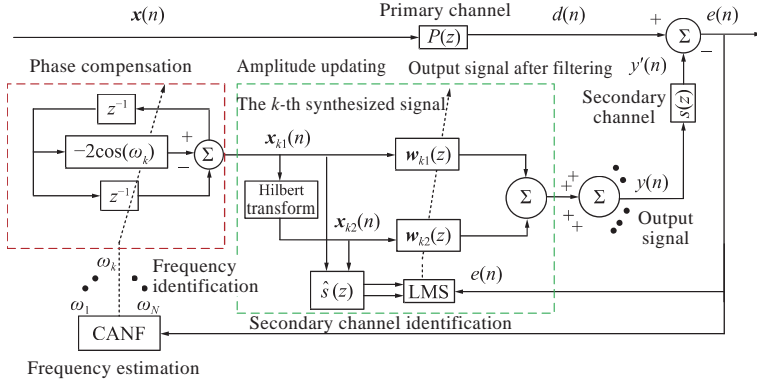


Fig. 3 Multi-line spectrum feedback control algorithm

secondary channel are unknown, and hence offline identification is required for the secondary channel before control. The filter is modeled through finite impulse response (FIR) with the same  $M$ -order coefficient for estimation, and the obtained identification model is as follows

$$\hat{\mathbf{s}}(n) = [\hat{s}_0(n), \hat{s}_1(n), \dots, \hat{s}_{M-1}(n)]^T \quad (17)$$

where  $\hat{\mathbf{s}}(n)$  is the identified characteristic of the secondary channel. The filtering reference signal  $\hat{\mathbf{r}}_i(n)$  is

$$\begin{aligned} \hat{\mathbf{r}}_{i1}(n) &= \sum_{j=0}^{M-1} \hat{s}_j \mathbf{x}_{i1}(n-j) \\ \hat{\mathbf{r}}_{i2}(n) &= \sum_{j=0}^{M-1} \hat{s}_j \mathbf{x}_{i2}(n-j) \end{aligned} \quad (18)$$

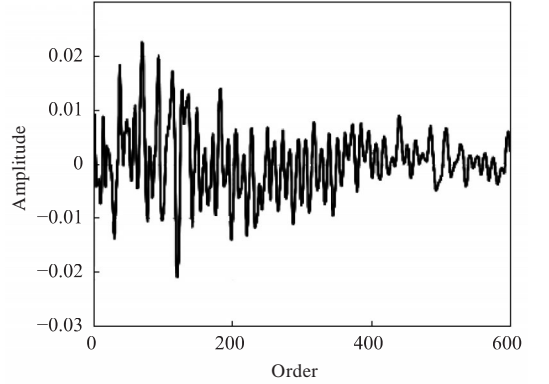
According to the least mean square (LMS) algorithm, the iterative formula for the weight coefficient  $\mathbf{w}_i(n)$  of the control filter is

$$\begin{aligned} \mathbf{w}_{i1}(n+1) &= \mathbf{w}_{i1}(n) - 2\mu_1 e(n) \hat{\mathbf{r}}_{i1}(n) \\ \mathbf{w}_{i2}(n+1) &= \mathbf{w}_{i2}(n) - 2\mu_2 e(n) \hat{\mathbf{r}}_{i2}(n) \end{aligned} \quad (19)$$

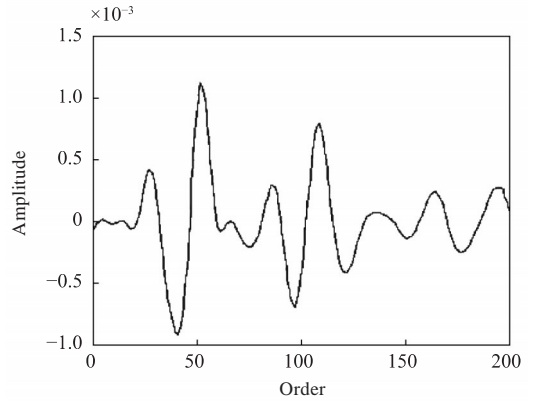
## 2 Simulation analysis

The performance of the narrow-band control algorithm for frequency estimation was verified by simulation. The data measured in the single-channel active vibration isolation experiment were converted into the coefficients of 600-level and 200-level transversal FIR filters, which were in turn taken as the impulse response functions of the primary and secondary channels. Fig. 4 shows the amplitude characteristics of those channels.

White noise with an SNR of 20 dB is superimposed on a fourth-harmonic signal with respective frequencies of 30, 37, 60, 110 Hz and the same amplitude of 1 to serve as a reference signal. The sampling rate is 10 kHz, and each LMS filter is a 300-level transversal FIR filter. The iteration step sizes of both algorithms are adjusted to their optimal values, and the level  $N$  of the cascaded adaptive notch



(a) Amplitude characteristic curve of the primary channel



(b) Amplitude characteristic curve of the secondary channel

Fig. 4 Transfer function amplitude of the primary and secondary channels

filters is set to 4. The acceleration response to the residual signal is adopted as the evaluation criterion, and the signal's amplitude drop before and after the implementation of the active control is the vibration isolation effect. Fig. 5–Fig. 9 show the simulation results of the algorithms.

The FXLMS algorithm in Fig. 5 does not converge completely until its 60 000-th iteration. The residual signal is reduced by 75% in the time domain. The vibration line spectra at 30, 37, 60, 110 Hz undergo respective amplitude attenuation of merely 7.17, 11.95, 0, 8.81 dB in the frequency domain, which indicates that the control effect is poor. Fig. 6

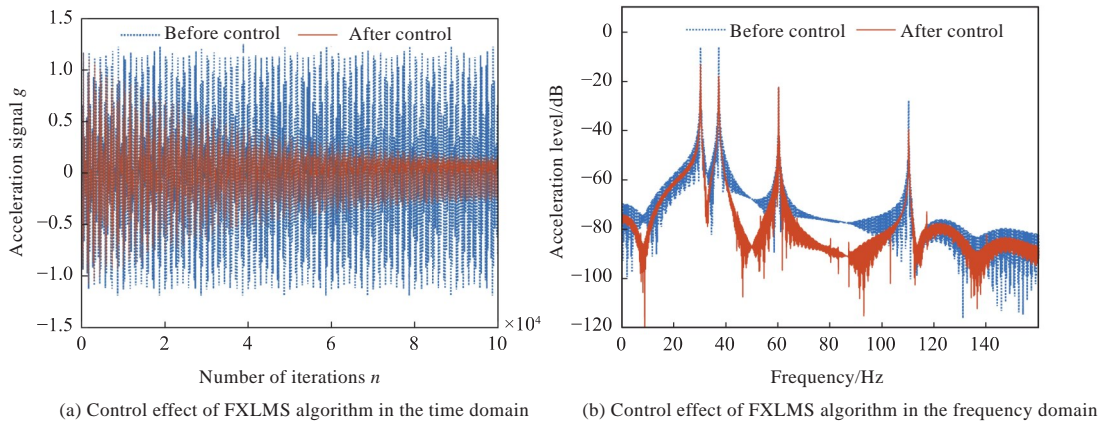


Fig. 5 Simulation results of the FXLMS algorithm

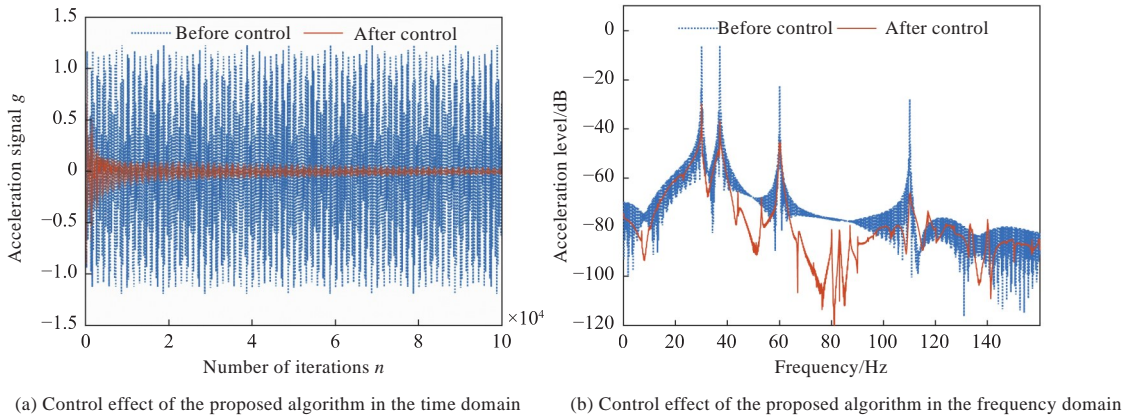


Fig. 6 Simulation results of multi-line spectrum feedback control algorithm

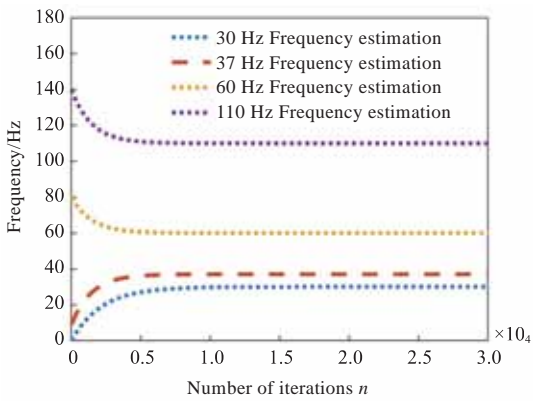


Fig. 7 Frequency estimation diagram of vibration line spectrum

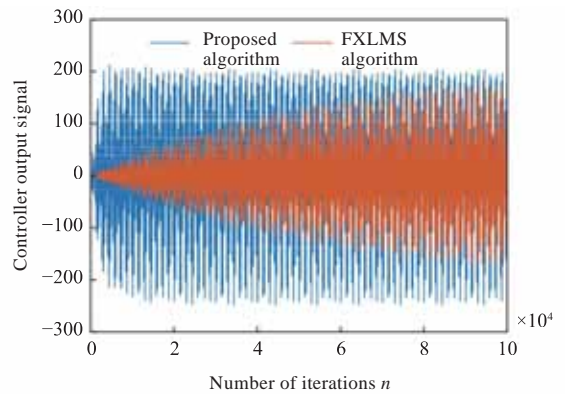


Fig. 9 Output signals under the proposed algorithm and the FXLMS algorithm

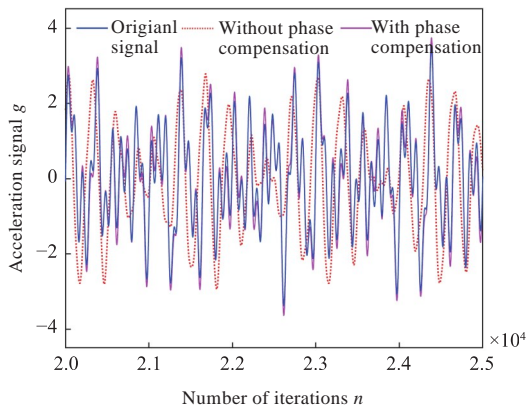


Fig. 8 Time history curves of the original signal and synthesized signal before and after phase compensation

Table 1 Vibration attenuation by the two algorithms in simulation

| Vibration line spectrum/Hz | Attenuation by the FXLMS algorithm/dB |               | Attenuation by the feedback algorithm/dB |               |
|----------------------------|---------------------------------------|---------------|--|---------------|
|                            | Before control                        | After control | Before control                           | After control |
| 30                         | -6.34                                 | -13.51        | -6.34                                    | -29.79        |
| 37                         | -6.12                                 | -18.07        | -6.12                                    | -36.64        |
| 60                         | -22.5                                 | -22.5         | -22.5                                    | -45.37        |
| 110                        | -27.97                                | -36.78        | -27.97                                   | -66.05        |

shows that the line spectrum feedback control algorithm exhibits a better control effect on multi-frequency signals, as the residual signal completes the convergence after 20 000 iterations and the amplitude is reduced by more than 90%. In the frequency domain, the amplitudes of the line spectra at 30, 37, 60, 110 Hz are reduced by 23.45, 30.52, 22.87, 38.08 dB respectively. Table 1 reports the attenuation of each vibration line spectrum.

Fig. 7 demonstrates that the algorithm accomplishes accurate identification of frequency information after 5 000 iterations and achieves real-time frequency tracking. Fig. 8 shows the time history curves of the original signal and the synthesized signal. It can be observed that a phase difference is between the synthesized signal and the original signal when the phase is not compensated while the synthesized signal better matches the original signal after compensation. Fig. 9 shows the controller output signal in both cases of the proposed algorithm and the FXLMS algorithm. According to the figure, the FXLMS algorithm exhibits a poor convergence effect with widely-distributed eigenvalues of the auto-correlation matrix of the input signal for multi-frequency excitation. In contrast, the multi-line spectrum feedback control algorithm puts signals with different frequencies into parallel controllers for processing and enjoys a better control effect according to the simulation results.

### 3 Active vibration isolation experiment

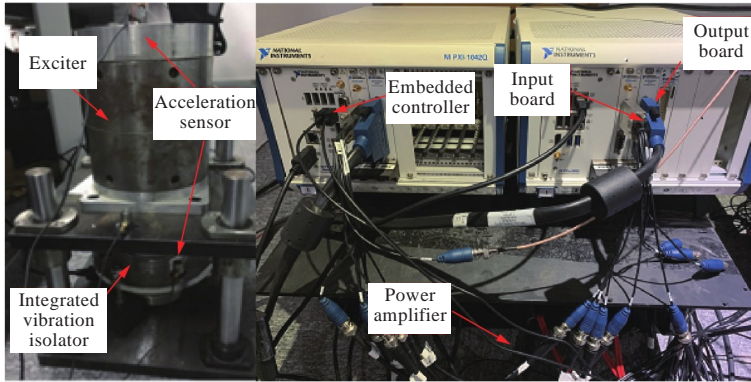
To verify the feasibility of the algorithm, NI PXI carrying an RT system is employed in this study to perform an active vibration isolation experiment. The experimental objects are an electromagnetic vibration exciter and additional counterweights that are used to simulate small-sized and medium-sized mechanical equipment. The equipment mainly includes the NI LabVIEW control system, Copley Xenus servo driver, PCB acceleration sensor, electromagnetic vibration exciter, integrated active and passive vibration isolator, and WYK-20040K constant voltage and current DC power supply. The integrated active and passive vibration isolator, which is self-developed, exhibits a linear relationship between the output force and the input current within a low-frequency excitation range. The experimental site and its schematic diagram are shown in Fig. 10. The experimental bench is divided into upper and

lower layers, with the upper layer being equipped with an electromagnetic exciter and the lower plate being fixed on the ground. Column guide rails are placed at the four corners of the lower plate, and a slip fit between the upper plate and the column is achieved through ball bearings. The installation of the integrated vibration isolator to the upper and lower plates is fixed by bolts.

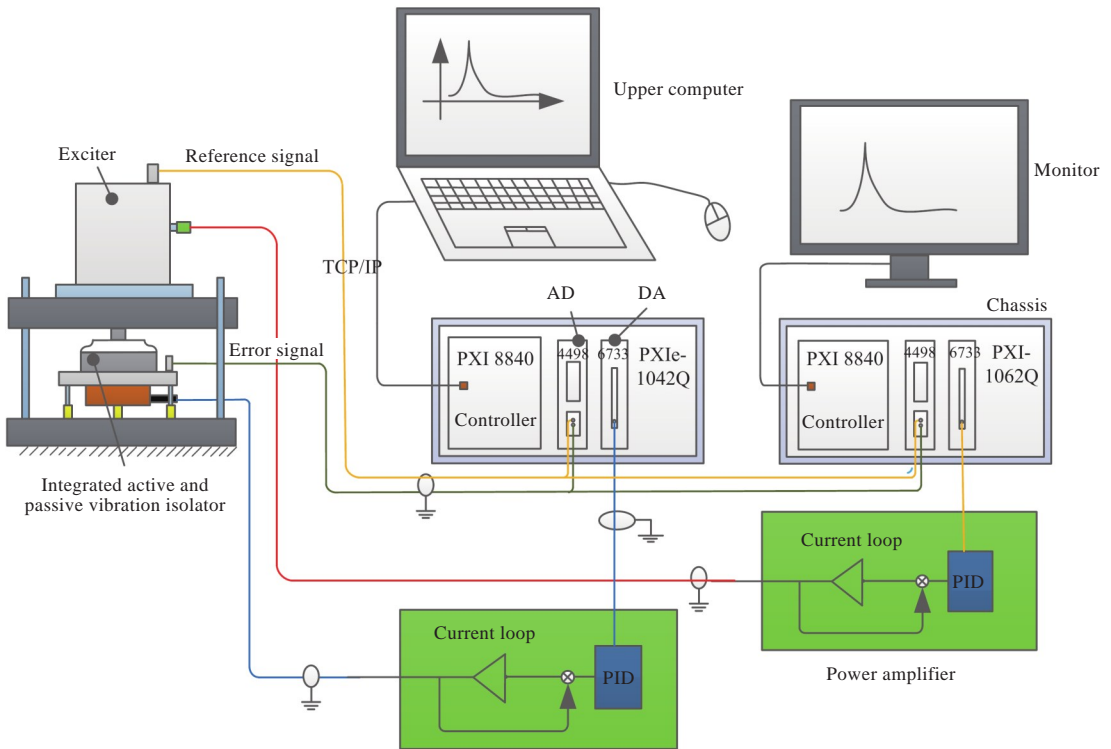
The acceleration sensors collect the excitation signal from the vibration source and the lower layer error signal (specifically, the signal from the vibration source is the reference signal for the FXLMS algorithm, and the lower layer error signal is the residual vibration). These signals then enter the PXI 8840 adaptive controllers through the PXI 4498 AD acquisition boards. The output control signals enter the power amplifiers through the PXI 6733 DA output boards and then drive the integrated active and passive vibration isolator to generate secondary vibration and thereby suppress primary vibration. The upper computer is connected to the PXIe-1042Q chassis by the TCP/IP communication line, and the algorithm program is configured to the lower computer to control the actuator's output force. PXI-1062Q controls the operation of the vibration exciter and the acquisition of vibration signals for real-time monitoring and post-processing.

A fourth-harmonic signal with respective frequencies of 30, 37, 60, 110 Hz is produced by the signal generator to serve as the initial excitation signal. All control filters have a length of 300 levels, and the iteration step size of each algorithm is adjusted to the optimal value. In particular, the sampling frequency is set to 10 kHz, which not only satisfies the sampling theorem but also ensures real-time signal tracking. A Butterworth band-stop filter is designed in the experiment to filter out the 50 Hz and 100 Hz power-line interferences in the signals collected by the AD boards. The acceleration response collected by the lower layer error signal sensor is employed as the evaluation criterion, and the signal's amplitude drop before and after the implementation of the active control is the vibration isolation effect. Fig. 11 and Fig. 12 demonstrate the respective control effects in the time domain and frequency domain.

The residual vibration signal obtained from Fig. 11(a) converges within 6 s after the implementation of the control, with a slow convergence speed and an amplitude reduction of merely 70%. Fig. 11(b) reveals amplitude attenuation of 11.28, 5.03, 5.33,

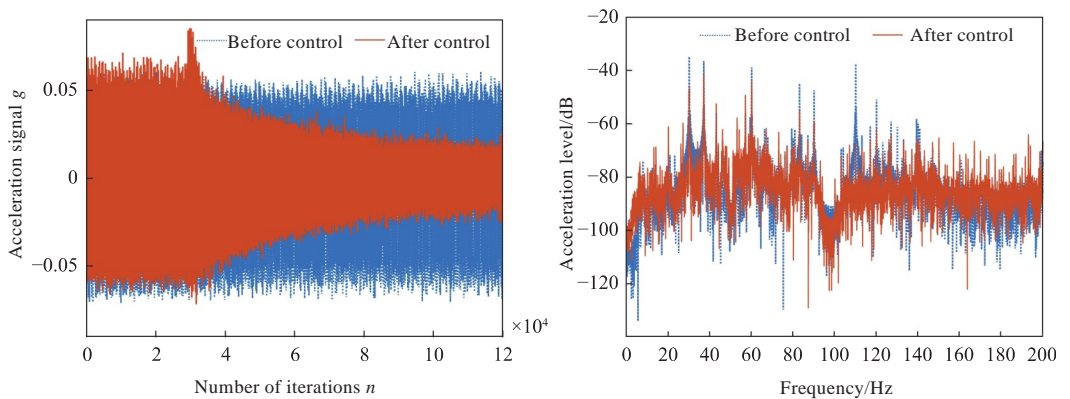


(a) Test site for active vibration isolation experiment



(b) Schematic diagram of active vibration isolation experiment

Fig. 10 Test site for active vibration isolation experiment and its schematic diagram



(a) Control effect of FXLMS algorithm in the time domain

(b) Control effect of FXLMS algorithm in the frequency domain

Fig. 11 Experimental results of the FXLMS algorithm

29.92 dB for the vibration line spectra at 30, 37, 60, 110 Hz, respectively, in the frequency domain. In particular, the control effects on the 30 Hz and 110 Hz

line spectra are excellent while those on the 37 Hz and 60 Hz line spectra are poor. The residual vibration signal obtained from Fig. 12(a) achieves con-

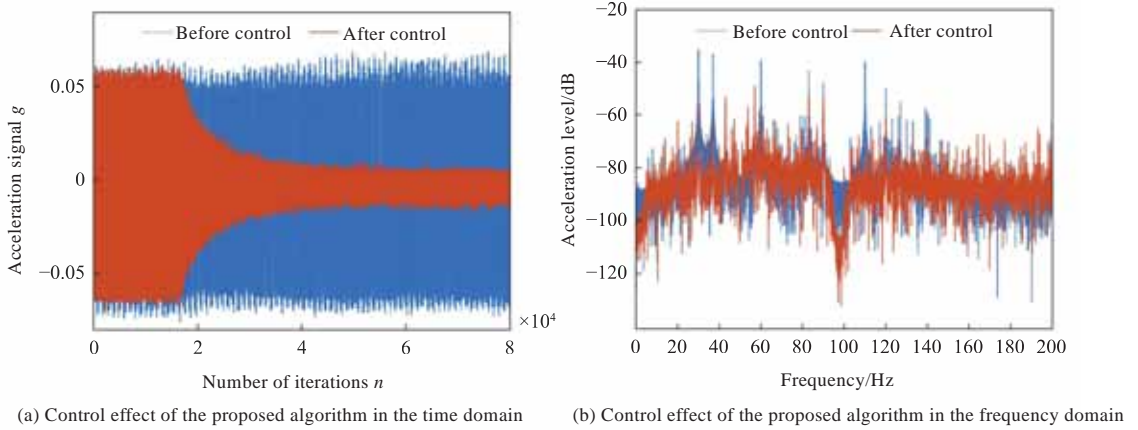


Fig. 12 Experimental results of the proposed algorithm

vergence within 2 s after the control is implemented, with a fast convergence speed and an amplitude reduction of 90%. Fig. 12(b) witnesses amplitude attenuation of 19.91, 25.93, 20.28, 31.39 dB for the vibration line spectra at 30, 37, 60, 110 Hz, respectively, in the frequency domain, and the control effects prove to be excellent. The attenuation of each vibration line spectrum is shown in Table 2. The effectiveness of the proposed algorithm is verified by a multi-line spectrum active vibration isolation experiment.

**Table 2 Comparison of vibration attenuation by two algorithms in the experiment**

| Vibration line spectrum/Hz | Attenuation by the FXLMS algorithm/dB |               | Attenuation by the feedback algorithm/dB |               |
|----------------------------|---------------------------------------|---------------|--|---------------|
|                            | Before control                        | After control | Before control                           | After control |
| 30                         | -35.1                                 | -46.38        | -35.1                                    | -55.01        |
| 37                         | -36.46                                | -41.49        | -36.46                                   | -62.39        |
| 60                         | -38.88                                | -44.21        | -38.88                                   | -59.16        |
| 110                        | -37.51                                | -67.43        | -39.48                                   | -70.87        |

## 4 Conclusions

A multi-line spectrum feedback control algorithm has been proposed to deal with the problems of multi-line spectrum vibration and reference signal mismatch. To start with, the error signal passed through cascaded adaptive notch filters, and the notch filter parameters were updated according to the adaptive algorithm to estimate multiple signal frequencies. Then, each reference signal was synthesized through phase compensation, and the Hilbert transform was applied to the signal to obtain another reference signal. Finally, the signals entered the parallel controllers to complete line spectrum control.

Accurate identification of 30, 37, 60, 110 Hz signals was implemented through the simulation and experiment of the proposed algorithm, and reliable reference signals were synthesized before they entered the algorithm. Moreover, amplitude attenuation of 20–40 dB for each line spectrum was achieved.

The proposed algorithm solves the problems of reference signal mismatch and multi-line spectrum vibration in vibration control, thereby effectively weakening and suppressing the transmission of low-frequency vibration energy.

## References

- [1] ZHU S J, LOU J J, HE Q W, et al. Vibration theory and vibration isolation [M]. Beijing: National Defense Industry Press, 2006 (in Chinese).
- [2] CHEN S Q, WANG Y, WEI C C, et al. An active vibration isolation control method under excitation of multi-line spectra [J]. Journal of Vibration and Shock, 2012, 31 (23): 128–131, 190 (in Chinese).
- [3] LI Y, HE L, SHUAI C G, et al. Improved hybrid isolator with maglev actuator integrated in air spring for active-passive isolation of ship machinery vibration [J]. Journal of Sound and Vibration, 2017, 407: 226–239.
- [4] NIU N, LIU Z, SUN L L. Modeling and analysis of decentralized intermediate mass hybrid vibration isolation system considering actuator output constraints [J]. Chinese Journal of Ship Research, 2019, 14 (6): 155–163 (in Chinese).
- [5] ELLIOT S J. Signal processing for active control [M]. London: Academic Press, 2001.
- [6] ZHAO H L, XU J, LI X D, et al. A modified algorithm of the active noise control system based on frequency-selective filter [J]. Acta Acustica, 2004, 29 (6): 499–506 (in Chinese).
- [7] LI Y, HE L, SHUAI C G. MIMO Fx-Newton narrow-band algorithm and experiment of active vibration isolation on diesel generator [J]. Acta Acustica, 2015, 40 (3): 391–403 (in Chinese).

- [8] GAO W P, HE G, LIU S Y, et al. Adaptive vibration control method based on wavelet packet transform [J]. Control and Decision, 2021, 36 (1): 83-89 (in Chinese).
- [9] ZHANG Z Y, WANG J F, ZHOU J P, et al. Adaptive vibration control with tracking filters [J]. Journal of Vibration and Shock, 2009, 28 (2): 64-67 (in Chinese).
- [10] ZHAI X J, ZHOU B. An improved interpolated FFT algorithm for harmonic analysis [J]. Proceedings of the CSEE, 2016, 36 (11): 2952-2958 (in Chinese).
- [11] WANG H, SUN H L, SUN Y P, et al. A narrowband active noise control system with a frequency estimation algorithm based on parallel adaptive notch filter [J]. Signal Processing, 2019, 154: 108-119.
- [12] DAI W H, QIAO C J, WANG Y K, et al. Adaptive cascaded notch filter for frequency estimation of multiple sinusoids [C]//Proceedings of the 2nd International Conference on Wireless Communication and Sensor Network. Changsha: World Scientific, 2016: 138-144.
- [13] SIRDI N K M, MONNEAU A, NAAMANE A. Adaptive notch filters for prediction of narrow band signals [C]//Proceedings of the 7th IEEE International Conference on Systems and Control (ICSC). Valencia, Spain: IEEE, 2018.
- [14] XIAO Y, MA L, KHORASANI K, et al. A new robust narrowband active noise control system in the presence of frequency mismatch [J]. IEEE Transactions on Audio, Speech, and Language Processing, 2006, 14 (6): 2189-2200.

# 反馈式多线谱主动隔振控制算法研究

张庆伟<sup>1</sup>, 俞翔<sup>\*2</sup>, 杨理华<sup>3,4</sup>

1 海军工程大学 动力工程学院, 湖北 武汉 430033

2 海军工程大学 舰船与海洋学院, 湖北 武汉 430033

3 海军潜艇学院 动力操纵系, 山东 青岛 266199

4 中国科学院 声学研究所 噪声与振动重点实验室, 北京 100190

**摘要:** [目的] 针对振动控制中多频激励的传统自适应滤波算法控制效果不佳, 以及工程中传感器不易安装和通道耦合等原因导致参考信号失配的问题, 提出一种反馈式多线谱控制算法。 [方法] 首先, 使误差信号通过级联自适应陷波器, 并根据自适应算法更新陷波器参数来估计多个信号频率; 然后, 合成各参考信号, 对相位进行补偿, 通过 Hilbert 变换得到另一路参考信号; 最后, 进入并行控制器完成幅值更新, 实现振动控制。 [结果] 仿真和试验结果表明, 该算法能够精确估计频率信息, 合成可靠参考信号, 对 30, 37, 60 和 110 Hz 线谱均取得了 20~40 dB 能量衰减。 [结论] 该算法较好地解决了振动控制中参考信号失配和多线谱振动的问题, 有效减弱和抑制了低频振动能量传递。

**关键词:** 多频激励; 参考信号失配; 主动隔振; 振动控制; 自适应陷波器; 频率估计; Hilbert 变换